HHS Public Access

Author manuscript

*Virology*. Author manuscript; available in PMC 2018 December 01.

Published in final edited form as:

*Virology*. 2017 December ; 512: 234–245. doi:10.1016/j.virol.2017.09.025.

# Infectivity of Sf-rhabdovirus variants in insect and mammalian cell lines

**Ajay B. Maghodia**[1] and **Donald L. Jarvis**[1,2,*]

[1]GlycoBac, LLC, Laramie, WY 82072

[2]Department of Molecular Biology, University of Wyoming, Laramie, WY 82071

## Abstract

Sf-rhabdovirus was only recently identified as an adventitious agent of *Spodoptera frugiperda* (Sf) cell lines used as hosts for baculovirus vectors. As such, we still know little about its genetic variation, infectivity, and the potential impact of variation on the Sf-rhabdovirus-host interaction. Here, we characterized Sf-rhabdoviruses from two widely used Sf cell lines to confirm and extend information on Sf-rhabdovirus variation. We then used our novel Sf-rhabdovirus-negative (Sf-RVN) Sf cell line to assess the infectivity of variants with and without a 320 bp X/L deletion and found both established productive persistent infections in Sf-RVN cells. We also assessed their infectivity using heterologous insect and mammalian cell lines and found neither established productive persistent infections in these cells. These results are the first to directly demonstrate Sf-rhabdoviruses are infectious for Sf cells, irrespective of the X/L deletion. They also confirm and extend previous results indicating Sf-rhabdoviruses have a narrow host range.

### Keywords

Sf-rhabdovirus; Adventitious viruses; Insect cells; Baculovirus expression system

## 1. Introduction

The baculovirus-insect cell system (BICS) has been used as a recombinant protein production platform to facilitate basic biomedical research for over three decades (Jarvis, 2009; Kost et al., 2005). More recently, it also has emerged as a commercial biologics manufacturing platform (Felberbaum, 2015). The BICS is a binary system consisting of a recombinant baculovirus vector, which encodes the protein of interest and provides the transcriptional machinery, and its insect cell host, which provides the translational and

*Corresponding author. Department of Molecular Biology, University of Wyoming, Laramie, WY, USA. Tel.: +1-307-766-4282. dljarvis@uwyo.edu.

**Declaration of interest**

ABM is an employee and DLJ is the President of GlycoBac, LLC, which is providing Sf-RVN cells under commercial agreements, and both are co-inventors on a GlycoBac patent application focused on the Sf-RVN cells utilized in this study.

processing machinery needed to produce the protein of interest. Cell lines derived from the fall armyworm, *Spodoptera frugiperda* (Sf) are among the most commonly used hosts in the BICS. The first Sf cell line described in the literature was derived from pupal ovaries, designated IPLB-SF-21AE and is commonly known as Sf21 (Vaughn et al., 1977). This cell line was used to isolate a subclone, which was designated Sf9 (Summers and Smith, 1987) and is widely used for research purposes today. Subsequently, Sf9 ATCC CRL-1711 lot 5814 ($Sf9^{L5814}$) was used to isolate Sf900+, an evolved derivative that was commercialized as *expres*$SF^{+}$ and is now used as the host in Protein Sciences Corporation's baculovirus expression system (BEVS) platform technology (Adams, 2017; Hashimoto et al., 2017; Smith et al., 2011).

In 2014, investigators at the U.S. Food and Drug Administration Center for Biologics Evaluation and Research reported Sf21 cells obtained from Invitrogen (Carlsbad, CA) and Sf9 cells obtained from Invitrogen and ATCC (Manassas, VA; CRL-1711 lot 58078522) are contaminated with an adventitious viral agent (Ma et al., 2014). Based on its negative stranded RNA genome, genome organization, and sequence, this agent was classified as a novel rhabdovirus, which is now known as Sf-rhabdovirus. Like all other rhabdoviruses, Sf-rhabdovirus encodes five conserved proteins, including nucleocapsid (N), phosphoprotein (P), matrix (M), glycoprotein (G), and polymerase (L; Fig. 1). Like many other rhabdoviruses, the original Sf-rhabdovirus harbored by Sf9 cells also encodes a non-conserved sixth protein (X) of unknown function (Fig. 1). Since the original discovery of this agent, other investigators have confirmed the presence of Sf-rhabdoviral RNA sequences in Sf9 (Haynes, 2015; Maghodia et al., 2016) and $Sf9^{L5814}$ (Hashimoto et al., 2017) cells. Thus, Sf-rhabdovirus is now widely recognized as a common contaminant of at least some Sf cell lines used as hosts for baculovirus-mediated recombinant protein production. This is important because Sf cells are being used not only for research purposes, but also to manufacture products approved for human clinical applications, as noted above. These include Dendreon's Sipuleucel T (PROVENGE®), which is an immunomodulator for treatment of late stage prostate cancer (Plosker, 2011), and Protein Science Corporation's Flublok®, which is a recombinant influenza viral vaccine (Cox and Hollister, 2009).

While the mere presence of an adventitious viral agent in at least some Sf cells raises obvious concerns, Sf-rhabdovirus infectivity has not been directly demonstrated, and this unknown is amplified by the existence of Sf-rhabdovirus variants with potentially significant genetic differences (Fig. 1). Ma and coworkers (2014) originally noted a difference in the Sf rhabdovirus L coding sequences detected in Sf9 (Fig. 1A) and Sf21 (Fig. 1E) cells, which consists of a six bp indel encoding a two amino acid difference in a non-conserved region of the viral RNA-dependent RNA polymerase. Haynes (2015) identified even more dramatic differences in the Sf-rhabdovirus sequences identified in their Sf9 cells, including a longer 3'-leader sequence and a 320 bp deletion starting in the X open reading frame and extending downstream into the X/L intergenic region (Fig. 1B). This same 320 bp deletion was found in the Sf-rhabdovirus X and X/L sequences detected by Hashimoto and coworkers (2017) in $Sf9^{L5814}$ cells (Fig 1C).

The detection of the full suite of RNA sequences representing a consensus rhabdoviral genome in various Sf cell lines lacking any obvious cytopathology suggests one or more Sf-

rhabdoviruses have established inapparent, persistent infections in these cells. The identification of particles with rhabdovirus-like morphology in concentrated Sf9 cell-free supernatants (Ma et al., 2014) further suggests these infections can be productive. However, in their recent study of Sf-rhabdovirus in $Sf9^{L5814}$ cells, Hashimoto and coworkers (2017) detected no particles with rhabdovirus-like morphology or size. They noted the Sf-rhabdovirus X/L sequences detected in these cells have the 320 bp deletion first described by Haynes (2015), and further noted this deletion eliminates the X and L gene transcriptional motifs originally predicted by Ma and coworkers (Hashimoto et al., 2017). Thus, this 320 bp X/L deletion would be expected to impair or prevent L gene transcription, which would be expected to block Sf-rhabdoviral replication because the L gene encodes the viral RNA-dependent RNA polymerase. However, the actual impact of the 320 bp X/L deletion remains unclear. While this deletion clearly includes the X/L intergenic transcriptional stop/start motif originally predicted by Ma and coworkers (2014), it is a putative motif whose function has never been experimentally confirmed. Hashimoto and coworkers (2017) also noted the absence of a full complement of Sf-rhabdoviral structural proteins in the 1.14 g/mL sucrose gradient fraction isolated from concentrated $Sf9^{L5814}$ cell-free supernatants, which would be expected to contain Sf-rhabdoviral particles. They found only N, truncated forms of N, P, and G, and cellular exosomal proteins, as well as Sf-rhabdoviral-specific RNA in this fraction. Finally, using an inverse PCR/nested PCR protocol with $Sf9^{L5814}$ cell DNA as the template, they detected three products that included Sf-rhabdoviral sequences encoding portions of the N, P, and L genes linked to Sf genomic sequences, indicating the $Sf9^{L5814}$ genome includes integrated DNA copies of Sf-rhabdoviral RNA sequences.

Together, these findings led Hashimoto and coworkers (2017) to conclude their study demonstrated the absence of rhabdovirus in $Sf9^{L5814}$ cells. Nevertheless, they detected Sf-rhabdovirus-specific RNAs in the intracellular and extracellular fractions of these cells. A potential explanation was virus-specific RNA(s) could be transcribed from genomically integrated DNA copies of Sf-rhabdoviral RNA and packaged, together with an incomplete set of Sf-rhabdoviral proteins, by cellular exosomes budding into the extracellular milieu. These processes could produce dense, non-viral particles containing Sf-rhabdovirus-specific RNAs with the capacity to mediate cell-to-cell transmission. Thus, this might explain the absence of particles with classical rhabdoviral morphology and size, the absence of a full suite of Sf-rhabdoviral structural proteins in the sucrose gradient fraction expected to contain those particles, and the source of the Sf-rhabdoviral sequences in the intracellular and extracellular fractions of $Sf9^{L5814}$ cells. However, this model cannot explain the authors' RT-PCR results, which showed total RNA from these cells included sequences representing 99.1% of the Sf-rhabdovirus genome, with genetic linkages between N-P, P-M, and X-L. The authors' model suggests these Sf-rhabdovirus-specific RNAs are derived from integrated viral sequences, but their inverse PCR/nested PCR results revealed integration of only partial, unlinked viral sequences representing ~30% of the viral genome (Hashimoto et al., 2017). In the final analysis, Hashimoto and coworkers' (2017) study on Sf-rhabdovirus in $Sf9^{L5814}$ cells produced some interesting new ideas on the nature of the Sf-rhabdovirus-host interaction in different cell lines, but it did not conclusively document the absence of Sf-rhabdovirus in $Sf9^{L5814}$ cells because neither their data nor their model can explain the source of RT-PCR products representing nearly the entire viral genome.

Considering the key questions surrounding this relatively new virus, we undertook this study to advance knowledge and understanding of Sf-rhabdovirus variation, infectivity, and the potential impact of genetic differences on the virus-host interaction. Our basic approach was to examine our Sf9 and Sf21 cells for Sf-rhabdovirus contamination, characterize the variants harbored by these cell lines, and examine their infectivity using various insect and mammalian cell lines. Our results confirmed Sf9 and Sf21 cells are contaminated with Sf-rhabdoviruses and confirmed the presence of variants with the previously described 6 bp indel in the L coding sequence (Ma et al., 2014), with and without the previously described 320 bp deletion in the X/L region (Hashimoto et al., 2017; Haynes, 2015). Our sequence analyses revealed multiple single nucleotide polymorphisms that can be used to distinguish the Sf-rhabdovirus variants harbored by different Sf cell lines. Interestingly, PCR analysis of genomic DNAs isolated from our Sf9, Sf21, and Sf-rhabdovirus-negative (Sf-RVN; (Maghodia et al., 2016) cells revealed none of the integrated Sf-rhabdoviral sequences detected by Hashimoto and coworkers (2017) in the $Sf9^{L5814}$ cell genome. Subsequently, we found the Sf-rhabdoviral variants produced by our Sf9 and Sf21 cells were both able to establish persistent, productive infections in Sf-RVN cells, which is the first direct evidence Sf-rhabdoviruses are infectious for Sf cells. These results also are the first to demonstrate Sf-rhabdoviruses can establish productive persistent infections in Sf cells, irrespective of the previously described 320 bp X/L deletion. Finally, we found neither Sf-rhabdovirus variant used in this study could establish a persistent infection in the heterologous insect or mammalian cell lines used in our study, extending previous data indicating Sf-rhabdovirus has a relatively restricted host range (Haynes, 2015; Ma et al., 2014).

## 2. Materials and methods

### 2.1. Cell culture

Sf-RVN and Sf9 cells were routinely maintained as shake-flask cultures at 28°C in ESF 921 medium (Expression Systems, Woodland, CA). Sf9, Sf21, and TN-368 cells were maintained as adherent cultures at 28°C in Grace's supplemented insect medium (TNMFH, Life Technologies Corporation, Grand Island, NY) containing 1% Pluronic® F-68 and 10% fetal bovine serum (Atlanta Biologicals, Inc., Flowery Branch, GA). S2R+ cells were maintained as an adherent culture at 28°C in Schneider's Drosophila medium (Invitrogen) containing 1% Pluronic® F-68 and 10% fetal bovine serum. Madin Darby Bovine Kidney (MDBK) and HeLa cells were maintained as adherent cultures at 37°C in GlutaMAX supplemented Dulbecco's modified Eagle's minimal essential medium (Invitrogen) containing 10% fetal bovine serum. After the addition of 10% fetal bovine serum, each growth medium was designated "complete" (C), as in C-TMNFH, C-Schneider's, or C-DMEM. As a commercial product, the composition of ESF 921 is proprietary. However, major differences between ESF 921 and C-TNMFH, which might be relevant to some results obtained in this study, are ESF 921 is a protein-free/serum-free growth medium, whereas C-TNMFH contains lactalbumin hydrolysate, yeastolate, and 10% fetal bovine serum.

### 2.2.Detecting and sequencing Sf-rhabdovirus genomic RNAs

Sf9 and Sf21 cells were grown as adherent cultures at 28°C in 75 $cm^2$ flasks and the cell-free C-TNMFH media were harvested by low speed centrifugation and filtered through a

0.22 mu;m filter (CELLTREAT Scientific, Shirley, MA). The filtrates were then layered onto 30% sucrose cushions and ultracentrifuged at 131,000 x g for 22 h at 4°C. Total RNA was extracted from the resulting pellets using an Omega Bio-tek E.Z.N.A. HP Total RNA Kit (Omega Bio-Tek, Inc., Norcross, GA), according to the manufacturer's protocol. The RNAs were then quantified and 1 mu;g samples were used as templates for cDNA synthesis with the ProtoScript II First Strand cDNA synthesis kit (New England Biolabs, Ipswich, MA) and an Sf-rhabdovirus negative strand-specific primer (NSP2; Table 1), according to the manufacturer's protocol. The reverse transcriptase was inactivated by incubating the reactions for 10 min at 85°C, the cDNAs were treated with RNaseH, and then equivalent amounts of each cDNA preparation were used for PCR's with Phusion® High-Fidelity DNA polymerase, HF reaction buffer (New England Biolabs), and various Sf-rhabdovirus gene-specific primers (Table 1). The reaction mixtures were incubated at 98°C for 1 min, cycled 35 times at 98°C for 30s, at 55–60°C for 30s, at 72°C for 1 min, and finally incubated at 72°C for 10 min. The primary PCR products were analyzed by agarose gel electrophoresis with ethidium bromide staining and amplimers of interest were then gel purified using HiBind DNA Mini Columns (Omega Bio-Tek, Inc., Norcross, GA), according to the manufacturer's protocol, directly sequenced (Genewiz, South Plainfield, NJ), and the sequences were assembled and aligned using Vector NTI 10.3.1 (Invitrogen). For some experiments, the RT-PCR assay described above was extended to include a secondary, nested PCR step, essentially as described previously (Maghodia et al., 2016), except we used the N-specific primer pairs NSP and NASP and NSeq1 and NSeq2 (Table 1) for the primary and secondary PCRs, respectively.

### 2.3. Probing for genomically integrated Sf-rhabdovirus- and Sf-rhabdovirus-like EVE-specific sequences

Total genomic DNA was isolated from Sf9, Sf21, and Sf-RVN cells, as described previously (Geisler and Jarvis, 2016), and aliquots were used for PCR's with Sf-rhabdovirus N-, P-, or L-specific or Sf-rhabdovirus N-, P-, or L-related EVE-specific primers. The primer sequences are shown in Table 1 and the PCR conditions were described above. The Sf-rhabdovirus-specific primers used for these experiments were designed to amplify the entire partial N, P, and L sequences previously reported to be integrated into the $Sf9^{L5814}$ cell genome (Hashimoto et al., 2017). The Sf-rhabdovirus N-, P-, or L-related EVE-specific primers were designed to amplify the entire N-, P-, and L-related EVEs previously described by Geisler and Jarvis (2016). PCRs with no template ($H_2O$) were used as negative controls and PCRs with the various genomic DNA templates and Sf glyceraldehyde phosphate dehydrogenase (GAPDH)-specific primers were used as positive controls. PCRs with total Sf cellular cDNA as the template were used as a second set of positive controls for the Sf-rhabdovirus N-, P-, and L-specific primers.

### 2.4. Assessing Sf-rhabdovirus infectivity

Sf-rhabdovirus infectivity was analyzed essentially as described previously (Ma et al., 2014). Briefly, media were collected from 95% confluent Sf9 or Sf21 cultures grown in C-TNMFH. Cell-free supernatants were prepared by low-speed centrifugation, filtered through a 0.22mu;m filter, and used as the Sf-rhabdoviral inocula, as described below.

To assess infectivity in Sf cells, replicate Sf-RVN cultures were seeded at a density of 2 x $10^6$ cells/25 $cm^2$ flask in ESF 921 medium. The cells were allowed to adhere for 1 h at 28°C, and then the media were removed and the cells were inoculated with 2.5 mL of either fresh medium (Mock) or the filtered cell-free supernatants from Sf9 or Sf21 cells cultured in C-TNMFH, which were prepared as described above. After inoculation, the cells were incubated for 2 h, fed with an additional 2.5 mL of fresh C-TNMFH, and incubated for another 24 h at 28°C. The cells in each flask from one set of cultures were harvested, washed three times with C-TNMFH, and pellets containing 1 x $10^6$ cells were prepared by low-speed centrifugation and used to isolate total RNA. The cells in each flask from the second set of cultures were washed three times and fed with fresh C-TNMFH, then incubated for another 48 h at 28°C. At that time, the cells in each flask were harvested, pellets containing 1 x $10^6$ cells were prepared by low-speed centrifugation, and the remaining cells were sub-cultured with a 1:5 split ratio in C-TNMFH medium, and seeded into fresh 25 $cm^2$ flasks. The resulting cultures were designated P1, incubated for 72 h, and then sampled and sub-cultured as described above. This process was repeated for a total of ten consecutive passages, with samples containing 1 x $10^6$ cells harvested by low-speed centrifugation at 72 h after each passage. In addition, at 72 h after the tenth passage, the cell-free supernatants were collected, filtered, and the filtrates were ultracentrifuged through 30% sucrose cushions, as described above. Finally, total RNA was extracted from both the low-speed cell and high-speed cell-free pellets, quantified, and 1 mu;g aliquots were used for cDNA synthesis with an Sf-rhabdovirus negative strand-specific primer (NSP2; Table 1), as described above. The cDNAs were treated with RNase-H and those prepared from the low-speed cell pellets were analyzed by PCR with Sf-rhabdovirus N-specific primers (Table 1), while those from the high-speed cell-free pellets were analyzed by PCR with Sf-rhabdovirus N, P, M, G, X or L-specific primers (Table 1), as described above.

To assess infectivity in heterologous insect or mammalian cell lines, replicate TN-368, S2R +, MDBK, or HeLa cell cultures were seeded at a density of 2 x $10^6$ cells/25 $cm^2$ flask in C-TNMFH, C-Schneider's, or C-DMEM media, respectively. Those cultures were used as hosts for Sf-rhabdovirus infectivity assays and samples were taken and analyzed by RT-PCR or RT-PCR/nested PCR, as described above, except these experiments were terminated at P3, rather than P10.

## 3. Results and discussion

### 3.1. Detection of Sf-rhabdoviruses in different Sf cell lines

In an effort to extend knowledge of the Sf-rhabdovirus variants harbored by different Sf cell lines, we prepared cell-free, conditioned media filtrates from Sf9 and Sf21 cells by low speed centrifugation and 0.22 m filtration, layered them onto 30% sucrose cushions, and produced pellets by ultracentrifugation, as described in Materials and methods and illustrated in Fig. 2A. We then extracted total RNA from the pellets and produced cDNAs using NSP2 (Table 1; Fig. 2A), which is an Sf-rhabdovirus negative strand-specific primer complementary to the first (3') 20 nucleotides of the genomic reference sequence (GenBank Acc. No. KF947078) reported by Ma and coworkers (2014). We used this primer for reverse transcription because we wanted to specifically detect genomic, negative stranded Sf-

rhabdovirus RNAs, with no contribution from any potential positive stranded RNA contaminants. This distinguished our study from all previously published studies on Sf-rhabdoviruses, which have utilized random hexamers, oligo(dT), or both for the reverse transcription step (Hashimoto et al., 2017; Haynes, 2015; Ma et al., 2014). This distinction is important because the negative stranded RNA specificity of our RT-PCR protocol focused our analysis on viral genomic RNAs and eliminated the complications of data interpretation associated with the potential presence of transcripts derived from Sf-rhabdovirus, Sf-rhabdovirus-related endogenous viral elements (EVES; Geisler and Jarvis, 2016), genomically integrated Sf-rhabdoviral sequences, or any other positive stranded, Sf-rhabdovirus-specific RNAs, such as replicative intermediates. After reverse transcription, we heat-inactivated the reverse transcriptase and completed the RT-PCR protocol using a broad selection of different Sf-rhabdovirus-specific primers (Table 1) to amplify the resulting cDNAs, as described in Materials and methods and illustrated in Fig. 2A.

Our initial RT-PCRs targeted Sf-rhabdoviral sequences spanning intergenic regions (Fig. 2A) because successful amplification of these sequences requires physical linkages between two adjacent viral sequence elements and/or coding sequences. This was another way to focus our analysis on genomic, negative stranded Sf-rhabdoviral RNAs, as these linkages do not exist in mRNAs derived from Sf-rhabdovirus, Sf-rhabdovirus-related EVEs, or integrated Sf-rhabdoviral sequences. The results showed RT-PCRs with RNAs from ultracentrifuge pellets of Sf9 or Sf21 cell-free media filtrates and primer pairs flanking the Sf-rhabdoviral 3'-leader/N, N/P, P/M, M/G, G/X, X/L, and L/5'-UTR junctions all produced amplimers of the expected sizes (Fig. 2B). These results indicated these ultracentrifuge pellets contained negative stranded Sf-rhabdoviral RNAs in which the 3' leader and N coding sequences, each pair of adjacent viral protein coding sequences, and the L coding and 5' UTR sequences, respectively, are physically linked. These results cannot be explained by the presence of any contaminating, Sf-rhabdovirus-related positive stranded RNAs, as explained above. Thus, we conclude the Sf9 and Sf21 cells used in this study are contaminated with Sf-rhabdoviruses and each sheds dense particles containing full length, negative stranded Sf-rhabdoviral RNAs into the extracellular milieu. These results confirm and extend previous results indicating Sf9 and Sf21 cells are contaminated with Sf-rhabdoviruses (Haynes, 2015; Ma et al., 2014).

### 3.2. Characterization of Sf-rhabdovirus variants harbored by different Sf cell lines

Our next goal was to characterize the Sf-rhabdovirus variants harbored by different Sf cell lines by directly sequencing the amplimers shown in Fig. 2B. The results showed the Sf9 cells used in our lab harbor a mixture of two major variants, with or without the previously described 6 bp L-gene insertion (Fig. 1D and data not shown; Ma et al., 2014). In addition, unlike the Sf9-rhabdovirus originally identified by Ma and coworkers (2014), our two major Sf9-rhabdovirus variants both have the 320 bp X/L deletion found in the Sf9-rhabdovirus identified by Haynes (2015; Figs. 1A–B, 1D, and data not shown).

Our results also showed the Sf21 cells used in our lab harbor an Sf-rhabdovirus with the same 6 bp L-gene insertion as the Sf21-rhabdovirus identified by Ma and coworkers (2014) and an intact X/L region, which was not previously examined (Fig. 1E and data not shown).

We subsequently performed RT-PCRs designed to produce a comprehensive set of overlapping fragments that could be used to assemble full-length sequences of the negative stranded Sf-rhabdoviral RNAs shed by the Sf9 and Sf21 cells used in this study. Again, the templates were total RNAs isolated from the ultracentrifuge pellets of cell-free media filtrates, as described in Materials and methods and illustrated in Fig. 2A. The reverse transcription primer was NSP2 (Table 1) and the PCR primer pairs were various Sf-rhabdovirus-specific primers designed using the reference sequence (Ma et al., 2014; GenBank Acc. No. KF947078; Table 1). These PCRs yielded two independent sets of multiple overlapping amplimers of the expected sizes spanning the entire negative stranded RNA genomes of the Sf-rhabdoviruses shed from Sf9 and Sf21 cells (data not shown). Each amplimer was directly sequenced and the sequences obtained using the two independent amplimer sets were assembled. Considering the particulate nature of the material used to isolate the RNA templates and the polarity of the NSP2 primer used for reverse transcription, we conclude these assemblies represent the full-length or nearly full-length sequences of the negative stranded RNA genomes of the major Sf-rhabdoviral variants shed into the extracellular milieu by these Sf cell lines. Hence, we deposited these viral genome sequences into GenBank as Sf9-rhabdovirus (Acc. No. MF536978) and Sf21-rhabdovirus (Acc. No. MF536979).

Because these Sf-rhabdoviral genome sequences were determined by directly sequencing PCR amplification products and the raw sequence data were not deconvoluted, they represent the most abundant quasi-species in the viral populations shed from the two different Sf cell lines. While this approach cannot provide information on Sf-rhabdovirus variation at the quasi-species level, it nevertheless revealed single nucleotide polymorphisms (SNPs) among the Sf-rhabdoviruses harbored by these cell lines. Specifically, the Sf9- and Sf21-rhabdovirus genome sequences identified in this study included 16 and 52 SNPs, respectively, relative to the Sf-rhabdovirus reference sequence (Ma et al., 2014; GenBank Acc. No. KF947078, Table 2). We cannot draw any definitive conclusions on the natural history of Sf-rhabdoviruses from these data. However, it is interesting to note the numbers of SNPs relative to the Sf9 viral reference strain reflect the relationships between these two different cell lines. For example, the Sf21-rhabdovirus sequence had more SNPs, which is consistent with the fact that it was derived from Sf21, the original Sf cell line (Vaughn et al., 1977), while the Sf9-rhabdovirus reference sequence was derived from the Sf21 subclone isolated about a decade later (Summers and Smith, 1987). Our Sf9-rhabdovirus sequence had fewer SNPs relative to the Sf-rhabdovirus reference sequence, which is consistent with the fact that it is derived from the same cell line as the virus used to generate the reference sequence. Interestingly, we observed only 16 SNPs, despite presumptively significant differences in the passage histories of the Sf9 cells used to produce the Sf-rhabdovirus reference sequence and the Sf9-rhabdovirus sequence described herein. While we do not know all the specific details required to compare their passage histories, these two distinct Sf9 cultures were independently maintained at Invitrogen and in our academic lab, respectively, and therefore most likely had significantly different passage histories. Finally, it is relevant to note that, in addition to the differences in their X/L and L gene sequences, the SNPs identified in this study could be useful as diagnostic markers to distinguish these two different Sf-rhabdoviral variants.

### 3.3. Analysis of Sf cell lines for genomically integrated Sf-rhabdovirus and Sf-rhabdovirus-related EVE sequences

As the last step in our current effort to assess the Sf-rhabdovirus sequences harbored by the Sf9 and Sf21 cells used in this study, we assayed genomic DNAs isolated from these cell lines by PCR with primers designed to amplify the entire Sf-rhabdoviral partial N, P, and L sequences detected in the $Sf9^{L5814}$ cell genome (Hashimoto et al., 2017). As one positive control, we assayed the same genomic DNAs by PCR with primers designed to amplify the entire Sf-rhabdovirus N-, P-, and L-related EVEs described by Geisler and Jarvis (2016). These assays serve as positive controls because the Sf-rhabdovirus-related EVEs, which are related to, but distinct from Sf-rhabdovirus sequences, are know to be integrated into Sf cell genomes. As another positive control, we assayed these genomic DNAs by PCR with Sf-GAPDH-specific primers. Finally, as a third positive control, we amplified a total Sf9 cell cDNA preparation using the Sf-rhabdoviral N-, P-, and L-specific primers. We observed no evidence of any amplification products when we used genomic DNAs from our Sf9 or Sf21 cells and primers designed to amplify the Sf-rhabdoviral sequences detected in the $Sf9^{L5814}$ genome by Hashimoto and coworkers (2017; Fig. 3A). In contrast, we observed strong amplification products of the expected sizes when we amplified Sf9 cDNA with the same Sf-rhabdovirus N-, P-, and L-specific primer pairs (Fig. 3A). We also observed strong products of the expected sizes when we amplified the Sf9 or Sf21 genomic DNAs with Sf GAPDH primers (Fig. 3A). Finally, we observed strong products of the expected sizes when we amplified Sf9 or Sf21 genomic DNAs with the Sf-rhabdovirus N-, P-, and L-related EVE specific primer pairs (Fig. 3B). These results strongly suggest the Sf-rhabdovirus sequences amplified using $Sf9^{L5814}$ genomic DNA are not found in the genomes of the Sf9 or Sf21 cells used in this study.

We should note these experiments also showed the Sf-rhabdoviral sequences identified in $Sf9^{L5814}$ genomic DNA are not integrated into the genome of Sf-RVN, which is the key cell line used in the next phase of this study. This is important because it supports and extends our previously published results indicating these cells neither contain nor shed any detectable Sf-rhabdovirus sequences. It also is consistent with the results of a comprehensive genomic and transcriptomic project and bioinformatics analysis, which indicated Sf-RVN cells have no viral contaminants (C. Geisler, submitted for publication).

### 3.4. Infectivity of Sf-rhabdovirus variants in Sf cells

Data indicating Sf9 and Sf21 cells can shed genetically different negative stranded Sf-rhabdovirus RNAs suggested the observed SNPs, differences in their L coding sequences, and differences in their X coding and X/L intergenic region sequences do not prevent any of these variants from establishing persistent, productive viral infections in these cells. It is worth noting the Sf9 cells used in our study were maintained as a suspension culture for 91 passages, tested multiple times, and found to be contaminated with Sf9-rhabdovirus at various passages throughout the course of the study. Similarly, the Sf21 cells used for this study were derived from a frozen stock prepared from passage three, which was the number of subcultures we performed after receiving a frozen stock with an unclear passage history in 1994. These observations suggest Sf-rhabdovirus has persisted as an Sf cell contaminant for a long time, through at least one documented subcloning step to produce Sf9 (Summers and

Smith, 1987), and certainly through many routine serial passages in different labs. Thus, Sf-rhabdovirus appears to be a common, transmissible contaminant of Sf cell lines. However, it has not been directly shown that Sf-rhabdovirus is infectious for Sf cells. Furthermore, we have no data on the impact of genetic variation, particularly the impact of the 320 bp X/L deletion, on Sf-rhabdovirus infectivity. This these questions prompted our next set of experiments, which were designed to directly examine the infectivity of different Sf-rhabdovirus variants in Sf cells.

Our basic approach was to use cell-free media filtrates from our Sf9 and Sf21 cultures, which were known to be contaminated with the Sf-rhabdoviral variants described above, to inoculate Sf-RVN, a novel Sf line that has no Sf-rhabdovirus (Maghodia et al., 2016). One day after inoculation, the Sf-RVN cells were extensively washed, returned to the incubator, and then samples were harvested and used to prepare cell lysates at various times post-inoculation. Duplicate Sf-RVN cultures inoculated with the same filtrates were serially subcultured through ten passages in parallel, every three days after inoculation, and cell lysates were prepared from samples harvested at the time of each passage. In addition, cell-free media filtrates and ultracentrifuge pellets were prepared when the experiment was terminated ten passages after inoculation. Finally, total RNA was isolated from each cell lysate and ultracentrifuge pellet and used for RT-PCRs with Sf-rhabdoviral N-specific or other Sf-rhabdoviral gene-specific primers, respectively, as described in Materials and methods.

The inoculum used for our initial Sf-rhabdoviral infectivity experiments was a cell free medium filtrate from an Sf9 culture maintained in ESF 921 (Expression Systems). As a control, we produced an ultracentrifuge pellet using a sample of this inoculum and showed it was positive for Sf-rhabdovirus RNA using N-specific RT-PCR (data not shown). Thus, we were surprised to find no evidence of Sf-rhabdovirus RNA in Sf-RVN cell lysates three passages after they were inoculated with this filtrate, even after extending the RT-PCR assay to include a secondary nested PCR step, as described in Materials and methods (data not shown). We considered Sf-rhabdoviral RNA-containing particles shed by the contaminated Sf9 cells into serum-free ESF 921 medium might be extremely unstable. So, we repeated the infectivity experiments using a cell free medium filtrate from the same Sf9 cells cultured in ESF 921 medium supplemented with 10% fetal bovine serum as the inoculum. Again, we found no evidence of Sf-rhabdovirus RNA in Sf-RVN cells three passages after inoculation, even with the ultrasensitive RT-PCR/nested PCR assay (data not shown). Finally, we repeated the infectivity experiments using a cell free medium filtrate from the same Sf9 cells cultured in C-TNMFH. These experiments produced the first direct evidence of Sf9-rhabdovirus infectivity, as we observed an amplification product of the expected size in primary RT-PCRs with total RNAs from Sf-RVN cell extracts prepared at various times after inoculation and N-specific primers (Table 1; Fig. 4A, upper panel). This amplimer was detectable 24 h post-inoculation and its intensity increased with time after inoculation, reaching a plateau at passage four and remaining at about this same level up to passage ten. An amplimer of the same size was obtained by RT-PCR with total RNA from the same Sf9 cells used to produce the original Sf-rhabdoviral inoculum, which served as the positive control for the assay (Fig. 4A, upper panel, Sf9). No amplimer was obtained by RT-PCR with total RNA from Sf-RVN cells inoculated with fresh C-TNMFH, which served as the

negative control for the assay (Fig. 4A, upper panel, Mock). Finally, amplimers of the expected sizes were obtained by primary RT-PCR with total RNA from an ultracentrifuge pellet produced using the Sf-RVN cell-free medium filtrate harvested ten passages after inoculation (Fig. 4A, lower panel). This extracellular particulate fraction was assayed by RT-PCR with a full set of Sf-rhabdovirus gene-specific primers designed to amplify each viral protein coding sequence. Direct sequencing showed each amplimer produced in these assays had not only the correct size, but also the correct sequence (data not shown).

As noted, these results provided the first direct evidence that Sf9 cells shed an infectious agent into the extracellular milieu, which can be transmitted to an Sf-rhabdovirus-negative Sf cell line. The steady increase in the intensity of the negative stranded N-specific amplimer from 24 h to passage four post-inoculation indicated the Sf9-rhabdoviral genome can replicate after being delivered to Sf-RVN cells. The plateau in the intensity of the negative stranded N-specific amplimer observed at passage four, together with its maintenance at about the same level through passage ten, indicated Sf9-rhabdovirus can establish a persistent infection in Sf-RVN cells. Finally, the detection of amplimers representing the full suite of Sf-rhabdovirus protein coding sequences by RT-PCR of the ultracentrifuge pellet from the Sf-RVN cell-free medium filtrate at ten passages after inoculation indicated the persistently infected cells shed negative stranded Sf-rhabdoviral RNA(s) in the form of a dense particle into the extracellular milieu.

We conclude Sf9-rhabdovirus is an infectious contaminant of the Sf9 cells used in this study and that it can be transmitted to naïve cells lacking any detectable Sf-rhabdovirus sequences, in which it can replicate and establish a persistent, productive infection. It is interesting to recall the cell free media filtrates from Sf9 cells cultured in ESF 921 or ESF 921 supplemented with 10% fetal bovine serum did not produce detectable Sf-rhabdovirus infections. This was surprising because we can routinely detect negative stranded Sf9-rhabdoviral sequences in ultracentrifuge pellets prepared from Sf9 cell-free media filtrates, irrespective of the medium used for their cultivation (data not shown). Despite the presence of these viral RNAs in all three types of cell-free media filtrates, only the filtrate from Sf9 cells cultured in C-TNMFH transmitted the infection to Sf-RVN cells. These latter cells were initially cultured in ESF 921, but fed C-TNMFH after inoculation. At this time, we cannot explain this result. Clearly, the addition of 10% fetal bovine serum to ESF 921, alone, did not yield an infectious Sf9 cell-free medium filtrate. Thus, we speculate some other component of C-TNMFH might be required, perhaps to stabilize the virus in the cell free medium or to facilitate the delivery of some form of viral negative-stranded RNA in the inoculum to the naïve Sf-RVN cell targets. Alternatively, perhaps some component of ESF 921 destabilizes those particles and/or inhibits their infectivity, neither of which can be prevented by the addition of fetal bovine serum.

We subsequently addressed the broader goal of assessing the potential impact of genetic variation on Sf-rhabdovirus infectivity by using the general approach described above to directly examine the infectivity of the Sf21-rhabdovirus in Sf cells. In short, the results obtained with both Sf-rhabdoviral variants were essentially identical. The negative stranded RNA genomes in the cell-free media filtrates from Sf21 cells were able to infect and replicate in Sf-RVN cells (Fig. 4B, upper panel) and to establish a persistent, productive

infection, as evidenced by the shedding of negative stranded Sf-rhabdoviral RNAs encoding all Sf-rhabdoviral proteins into the extracellular milieu (Fig. 4B, lower panel). We conclude the SNPs, differences in L coding sequences, and differences in X coding and X/L intergenic region sequences detected in the two different Sf-rhabdovirus variants used in this study do not impair or significantly influence their infectivity for Sf cells. These are the first results to demonstrate the utility of our Sf-RVN cells as a tool for the detection of Sf-rhabdoviruses and analysis of their infectivity.

### 3.5. Infectivity of Sf-rhabdovirus variants in heterologous insect cells

The purpose of our next set of experiments was to extend the experiments described above by examining Sf-rhabdovirus infectivity in heterologous insect cell lines. We used the same general approach described above, but used TN-368, a cell line derived from the lepidopteran insect *T. ni* (Hink, 1970), or S2R+, a cell line derived from the dipteran insect *D. melanogaster* (Yanagawa et al., 1998), as the hosts. We chose TN-368 because, like those derived from Sf, cell lines derived from *T. ni* are commonly used as hosts for recombinant protein production in the BICS. Accordingly, *T. ni* lines are commonly cultivated in parallel with Sf lines and potentially exposed to Sf-rhabdoviruses in labs using the BICS. We chose S2R+ because, like Sf, it is also derived from an insect and used for recombinant protein production, but *D. melanogaster* belongs to a different insect Order and S2R+ cells are not permissive for baculovirus infection. Thus, we used these two cell lines to determine if cell lines from evolutionarily close or distant insects, respectively, are susceptible to Sf-rhabdovirus infection. Briefly, the results of these experiments showed neither Sf-rhabdovirus variant used in our study could establish persistent, productive infections in either TN-368 (Fig. 5) or S2R+ (Fig. 6) cells. In these experiments, we added a secondary, nested PCR step to enhance the sensitivity of the RT-PCR analysis, as described in Materials and methods. This resulted in the detection of amplimers of the expected sizes when we used total RNAs isolated from TN-368 or S2R+ cells at early times after inoculation with both Sf-rhabdovirus variants, but not with negative controls from cells inoculated with fresh C-TNMFH (Mock, Figs. 5–6). However, the intensity of this amplimer did not increase with time nor did it persist beyond 1–2 passages after inoculation. These results suggested the amplimers observed at early time points were derived from Sf-rhabdovirus negative stranded RNAs present in some form in the inocula, which became tightly associated with the target cells, perhaps even internalized, but failed to replicate or establish persistent, productive infections in those cells. We conclude neither of the Sf-rhabdovirus variants used in this study can productively infect TN-368 or S2R+, the representative heterologous insect cell lines used in this study.

This conclusion is partially consistent with, but slightly different from the conclusions drawn from analogous experiments by Ma and coworkers (2014). These investigators assessed Sf9-rhabdovirus infectivity in High Five™ and SL2, which are also derived from *T. ni* and *D. melanogaster*, respectively. Their RT-PCR/nested PCR results revealed Sf-rhabdoviral-specific RNAs in these cells as late as 62 and 34 days post-inoculation, respectively. They concluded the cells were transiently infected and “Sf-rhabdovirus may potentially infect other insect cell lines” (Ma et al., 2014). However, the intensities of the Sf-rhabdovirus amplimers produced by their primary RT-PCRs also did not increase and actually faded with

time after inoculation, even though they remained detectable in High Five™ by nested RT-PCR for the duration of the experiment. Moreover, the signal obtained in their nested RT-PCRs with RNAs from concentrated High Five™ or SL2 cell-free media filtrates actually disappeared at 49 and six days post-inoculation, respectively, indicating neither cell line was productively infected. Thus, while we might agree Sf-rhabdoviruses can transiently infect or, at least, viral RNA in some form can become transiently associated with these cells, we do not think either data set supports the idea Sf-rhabdovirus can establish productive, persistent infections in these heterologous insect cell lines. As part of this discussion, we should highlight some specific methodological differences in our heterologous insect cell infectivity experiments, relative to those performed by Ma and coworkers (2014). First, we used different cell lines and Sf-rhabdoviruses. Second, we used an Sf-rhabdovirus negative strand-specific primer for reverse transcription, while Ma and coworkers (2014) used the iScript reaction mix, which contains a mixture of oligo(dT) and random hexamers as the primers. Thus, our RT-PCR/nested RT-PCR assays were restricted to the detection of negative stranded RNAs, while theirs would also detect positive stranded RNAs produced by transcription of Sf-rhabdovirus genomic RNAs. This latter technical difference is significant and could explain the longer persistence of L-specific amplimers observed by RT-PCR/nested PCR in Ma and coworkers (2014) High Five™ cell infectivity experiment.

### 3.6. Infectivity of Sf-rhabdovirus variants in mammalian and human cells

The purpose of the final set of experiments performed in this study was to extend our analysis of the host range of the Sf-rhabdovirus variants to include mammalian and human cell lines. Thus, we inoculated MDBK and HeLa cells with Sf9 or Sf21 cell-free C-TNMFH media filtrates, isolated total RNAs from cell lysates at various times and passages after inoculation, and assayed samples by RT-PCR and RT-PCR/nested PCR using Sf-rhabdovirus N-specific primers, as described above. Like the results obtained with the heterologous insect cell lines, the results of these assays revealed amplimers of the expected size, but only with total RNAs from MDBK (Fig. 7) and HeLa (Fig. 8) cells isolated at early times after inoculation. Again, the intensity of these amplimers did not increase with time after inoculation with filtrates from either cell line and they completely disappeared by one passage after inoculation. These results indicated negative stranded Sf-rhabdoviral RNAs present in some form in the inocula transiently associated with MDBK and HeLa cells, but failed to replicate and establish persistent infections in these cells.

We conclude the Sf-rhabdovirus variants examined in this study have relatively narrow host ranges and cannot establish persistent, productive infections in the mammalian or human cell lines used in this study. This conclusion is consistent with the conclusion drawn from the results of analogous experiments by Ma and coworkers (2014), which revealed no evidence of Sf-rhabdovirus RNAs beyond 2 days after inoculating several different mammalian or human cell lines with their Sf9-rhabdovirus.

## 4. Summary and perspectives

This study was designed to examine different Sf cell lines for Sf-rhabdoviruses, characterize their major genetic differences, and examine their infectivity’s and, in a coarse way, their

host ranges. The results confirmed and extended previous findings indicating various Sf lines are contaminated with Sf-rhabdoviruses and different Sf lines can harbor different Sf-rhabdovirus variants (Hashimoto et al., 2017; Haynes, 2015; Ma et al., 2014). The results also showed the Sf lines used in this study do not have integrated DNA copies of the Sf-rhabdoviral RNA sequences recently identified by inverse PCR/nested PCR analysis of genomic DNA from $Sf9^{L5814}$ cells (Hashimoto et al., 2017).

This study also produced the first direct evidence Sf-rhabdovirus is infectious for Sf cells. Moreover, it showed the Sf-rhabdovirus variants shed by Sf9 and Sf21 cells are both infectious for Sf cells, irrespective of genetic differences that included SNPs, L coding indels, and a 320 bp deletion spanning a portion of the X coding sequence and X/L intergenic region. The documented infectivity of Sf-rhabdovirus variants with the X/L deletion shows the X protein is dispensable for Sf-rhabdovirus infection and the 320 bp deletion does not preclude functional expression of the viral RNA-dependent RNA polymerase. This latter conclusion leads us to speculate the predicted transcriptional control element in the X/L intergenic region, which is included in this 320 bp deletion, was misidentified in the original Sf-rhabdovirus description (Ma et al., 2014). This does not reflect poorly on the investigators or their prediction, but rather, reflects the problems associated with using bioinformatically predicted functions to interpret downstream results. Our bioinformatics analyses suggest the actual X/L termination/reinitiation signal is likely located further downstream (C. Geisler, unpublished), but the quality of this prediction, like the quality of the first, will require experimental assessment.

More broadly, some of the results obtained in this study can be used to discuss ideas presented in the recent analysis of Sf-rhabdovirus contamination in $Sf9^{L5814}$ cells, which reportedly demonstrated “the absence of rhabdovirus in a distinct Sf9 cell line” (Hashimoto et al., 2017). For example, one of the authors’ arguments in support of this conclusion was the 320 bp X/L deletion in the Sf-rhabdovirus sequence they identified in $Sf9^{L5814}$ cells “eliminates the transcriptional motifs for genes X and L”. We now know this is incorrect because the Sf9-rhabdovirus characterized herein has the same deletion, but can infect Sf-RVN cells. In fact, none of the genetic differences between the Sf-rhabdovirus variants used in our study eliminated their infectivity for Sf cells. Therefore, if there is a viral genetic basis for the “absence of rhabdovirus” in $Sf9^{L5814}$ cells, it must be a novel difference that is not found in either of the variants used in our study.

Two other observations that supported Hashimoto and coworkers’ (2017) overall conclusion was they detected neither particles with rhabdovirus-like morphology nor a full complement of Sf-rhabdoviral proteins in the 1.14 g/mL sucrose gradient fraction isolated from $Sf9^{L5814}$ cell free supernatants. On the other hand, they did detect cellular exosomal markers, an incomplete set of Sf-rhabdovirus proteins or protein fragments, and Sf-rhabdoviral-specific RNAs in this fraction. Together with their inverse PCR/nested PCR evidence of genomically integrated Sf-rhabdovirus sequences, these data led the authors to propose Sf-rhabdoviral RNA(s) derived from integrated DNA copies of the negative stranded Sf-rhabdoviral RNA genome can be packaged, together with an incomplete set of Sf-rhabdoviral proteins, by cellular exosomes. This process could mediate the release of viral RNA(s) into the extracellular milieu in the form of dense particles with the capacity for cell-to-cell

transmission (Hashimoto et al., 2017). We agree some of the data obtained by Hashimoto and coworkers (2017) are consistent with this model. However, we do not agree this conclusively demonstrates the "absence of rhabdovirus" in $Sf9^{L5814}$ cells. The authors' inverse PCR/nested PCR results documented genomically integrated copies of incomplete, unlinked viral sequences representing only ~30% of the reference Sf-rhabdovirus genome. However, their RT-PCR results documented sequences in total $Sf9^{L5814}$ cell RNA representing 99.1% of the reference viral genome, as well as physical linkages between the N/P, P/M, and X/L sequences. We conclude there must be another source of these virus-specific RNA sequences in $Sf9^{L5814}$ cells and the simplest explanation might be these cells are contaminated with an Sf-rhabdovirus. This could be true whether or not they produce particles with classic, bullet shaped morphology and the correct size. In fact, we believe the authors' model presents an interesting and potentially important scenario in which exosomes capable of mediating Sf-rhabdoviral RNA externalization and cell-to-cell transmission could be, *a priori*, infectious contaminants. While biochemically distinct, one could argue they might be as important as a conventional Sf-rhabdoviral contaminant, in view of the authors' finding that exosomes can deliver a foreign, viral nucleic acid to naïve targets (Hashimoto et al., 2017).

In any case, the model discussed above cannot explain the infectious nature of the Sf-rhabdoviral RNAs in the particulate fraction of the cell free media filtrates from Sf9 and Sf21 cells, as demonstrated in this study. First, neither cell line had any detectable integrated DNA copies of Sf-rhabdovirus-specific sequences. Second, the particles released by the Sf9 and Sf21 cells used in this study contained full-length or nearly full-length, negative stranded Sf-rhabdoviral genomes with physical linkages between each of the predicted viral RNA regulatory elements and coding sequences. Due to the negative-stranded specificity of our RT-PCR assay, the amplimers obtained using total RNA from these particulate fractions cannot be derived from positive stranded rhabdoviral-related RNAs from any source, including integrated copies of the Sf-rhabdovirus genome or rhabdovirus-related EVES. Thus, the RNA component of the particulate extracellular fractions from these cells comprises negative stranded RNA rhabdoviral genomes that, when transmitted to naïve Sf cells, can replicate and establish persistent, productive infections. Absent any data on the protein composition of these particles, we cannot eliminate the possibility there are defects preventing the assembly and release of *bona fide* rhabdovirus-like particles from the persistently infected cells. We are investigating this possibility and, if we observe no particles with classic, bullet shaped morphology, we will certainly consider the exosome packaging and release elements of Hashimoto and coworkers' (2017) model might be correct and correctly applied to the Sf-rhabdoviral contaminants characterized in our study. On the other hand, we recognize these elements of Hashimoto and coworkers' (2017) model most likely do not apply to the contaminant originally identified by Ma and coworkers (2014), who found their contaminated Sf9 cells produced particles with classic, rhabdoviral morphology.

Finally, our results showed neither Sf-rhabdovirus variant tested could establish persistent infections in cell lines derived from other insects, mammals or humans. This extends previous work indicating Sf-rhabdovirus has a limited host range (Ma et al., 2014). This conclusion is obviously limited by the choice of Sf-rhabdovirus variants tested and the

conditions used for our infectivity studies, particularly the targeted host cell lines. Therefore, we still cannot ignore the potential biological risks associated with the presence of this adventitious viral contaminant in Sf cell lines, including lines that are currently being used to manufacture human products.

Accordingly, we believe it will be important for the community to directly assess Sf-rhabdovirus contamination in any Sf cell line used for commercial biologics manufacturing, including the Sf line used by Dendreon to manufacture Sipuleucel T (PROVENGE®) and the *expres*SF$^+$ line used by Protein Sciences Corporation to manufacture Flublok®. In this context, it is important to understand the relationship between Sf9$^{L5814}$ and *expres*SF$^+$ cells. Hashimoto and coworkers (2017) described the Sf9$^{L5814}$ cells used in their study as the "parent" of *expres*SF$^+$. Thus, they did not directly assess Sf-rhabdoviral contamination in their commercial *expres*SF$^+$ line, itself and whether or not one agrees with the authors' conclusions about Sf-rhabdovirus contamination of Sf9$^{L5814}$ cells, these conclusions cannot be directly applied to *expres*SF$^+$. In fact, this would be a particularly long leap of faith, as the patent describing the steps taken to establish Sf900+ (commercialized as *expres*SF$^+$) from ATCC CRL-1711 indicates this involved 85 passages and a "high level of cell mortality" creating selective pressure "needed for cells to undergo an evolutionary change" (Smith et al., 2011).

In closing, we should note we recognize the presence of Sf-rhabdovirus in any cellular substrate, including *expres*SF$^+$, does not preclude its use for biologics manufacturing. Instead, it demands excellent viral clearance measures, such as those that have been developed by Protein Sciences Corporation to ensure the safety of their products (Post, 2010). Accordingly, Protein Sciences has administered Flublok® to nearly 2500 adults in five randomized, placebo- or active-controlled human clinical trials and successfully documented its safety (Cox et al., 2015). Like other experts in the field, we are well aware of this track record and, therefore, it should be obvious our analysis of the recent publication on Sf-rhabdovirus contamination of Sf9$^{L5814}$ cells is intended to provide a scientific assessment of the results and conclusions presented therein (Hashimoto et al., 2017), not, in any way, to criticize any product commercialized by Protein Sciences Corporation.

## Acknowledgments

This work was supported by Awards Number R43 GM102982 and R44GM102982 from the National Institute of General Medical Sciences and R43 AI112118 from the National Institute of Allergy and Infectious Diseases, National Institutes of Health. The content is solely the responsibility of the authors and does not necessarily represent the official views of the National Institute of General Medical Sciences, National Institute of Allergy and Infectious Diseases, or National Institutes of Health. We acknowledge Drs. Christoph Geisler and Loy Volkman for helpful discussions and comments on the manuscript.

## References

Adams, D. BEVS platform technology. Protein Sciences Corporation. 2017. http://www.proteinsciences.com/BEVS.htm

Cox MM, Hollister JR. FluBlok, a next generation influenza vaccine manufactured in insect cells. Biologicals. 2009; 37:182–189. [PubMed: 19297194]

Cox MM, Izikson R, Post P, Dunkle L. Safety, efficacy, and immunogenicity of Flublok in the prevention of seasonal influenza in adults. Ther Adv Vaccines. 2015; 3:97–108. [PubMed: 26478817]

Felberbaum RS. The baculovirus expression vector system: A commercial manufacturing platform for viral vaccines and gene therapy vectors. Biotechnol J. 2015; 10:702–714. [PubMed: 25800821]

Geisler C, Jarvis DL. Rhabdovirus-like endogenous viral elements in the genome of Spodoptera frugiperda insect cells are actively transcribed: Implications for adventitious virus detection. Biologicals. 2016; 44:219–225. [PubMed: 27236849]

Hashimoto Y, Macri D, Srivastava I, McPherson C, Felberbaum R, Post P, Cox M. Complete study demonstrating the absence of rhabdovirus in a distinct Sf9 cell line. PLoS One. 2017; 12:e0175633. [PubMed: 28423032]

Haynes, J. Methods of detection and removal of rhabdovirus from cell lines. U.S.P.T.O. WO2015051255 A1. 2015.

Hink F. Established insect cell line from the cabbage looper, *Trichoplusia ni*. Nature. 1970; 226:466–467.

Jarvis DL. Baculovirus-insect cell expression systems. Meth Enzymol. 2009; 463:191–222. [PubMed: 19892174]

Kost TA, Condreay JP, Jarvis DL. Baculovirus as versatile vectors for protein expression in insect and mammalian cells. Nat Biotechnol. 2005; 23:567–575. [PubMed: 15877075]

Ma H, Galvin TA, Glasner DR, Shaheduzzaman S, Khan AS. Identification of a novel rhabdovirus in Spodoptera frugiperda cell lines. J Virol. 2014; 88:6576–6585. [PubMed: 24672045]

Maghodia AB, Geisler C, Jarvis DL. Characterization of an Sf-rhabdovirus-negative *Spodoptera frugiperda* cell line as an alternative host for recombinant protein production in the baculovirus-insect cell system. Prot Expr Purif. 2016; 122:45–55.

Plosker GL. Sipuleucel-T: in metastatic castration-resistant prostate cancer. Drugs. 2011; 71:101–108. [PubMed: 21175243]

Post PL. Safety testing and use of insect cells for recombinant protein production. PDA J Pharm Sci Technol. 2010; 64:396–418. [PubMed: 21502044]

Smith, GE., Knell, J., Vosnesensky, A. Spodoptera frugiperda single cell suspension cell line in serum-free media, methods of producing and using. U.S.P.T.O. 6,103,526. 2011.

Summers, MD., Smith, GE. Tx Ag Expt Stn Bull No 1555. 1987. A manual of methods for baculovirus vectors and insect cell culture procedures.

Vaughn JL, Goodwin RH, Thompkins GJ, McCawley P. The establishment of two insect cell lines from the insect *Spodoptera frugiperda* (Lepidoptera; Noctuidae). In Vitro. 1977; 13:213–217. [PubMed: 68913]

Yanagawa S, Lee JS, Ishimoto A. Identification and characterization of a novel line of Drosophila Schneider S2 cells that respond to wingless signaling. J Biol Chem. 1998; 273:32353–32359. [PubMed: 9822716]

## Highlights

- Confirms/extends genetic variation in Sf-rhabdoviruses from different cell lines.
- Directly demonstrates Sf-rhabdovirus infectivity for Sf cells.
- Shows Sf-rhabdovirus variants with 320 bp X/L deletion are infectious for Sf cells.
- Confirms/extends Sf-rhabdoviruses non-infectious for heterologous insect cell lines.
- Confirms/extends Sf-rhabdoviruses non-infectious for mammalian cell lines.

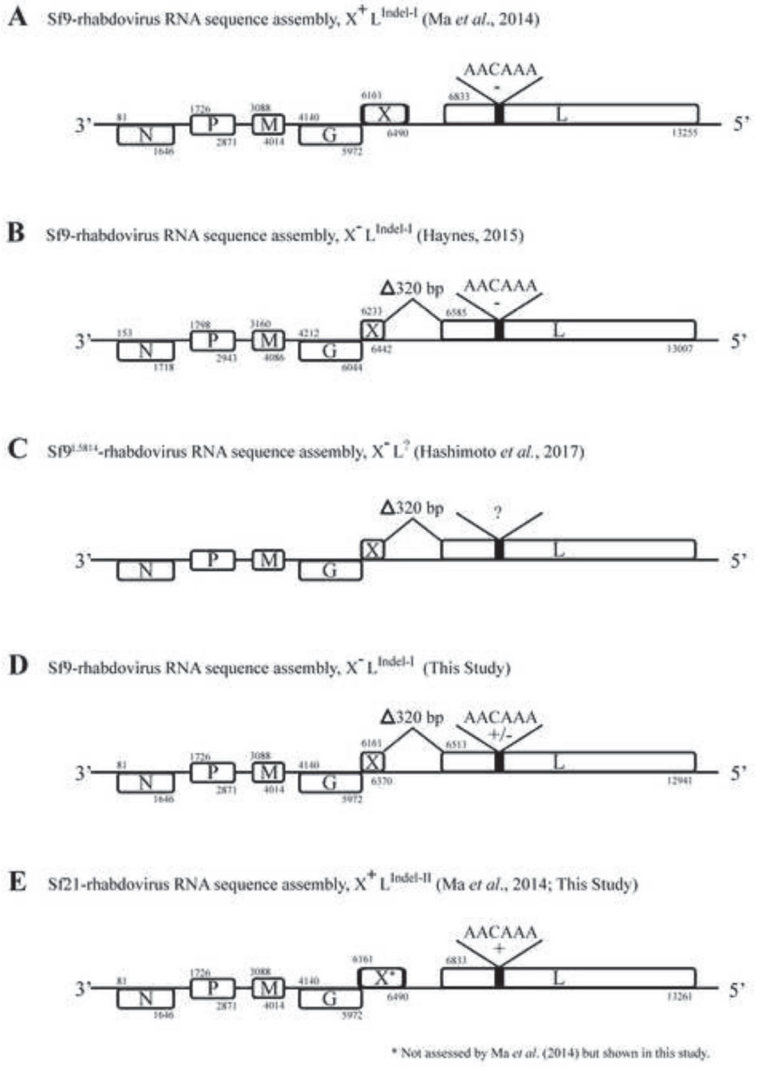


**Fig. 1.**

Sf-rhabdovirus RNA sequence assemblies. This Figure shows the Sf-rhabdovirus genome organization derived from RNA sequence assemblies and bioinformatics, as originally described by Ma and coworkers (2014) and highlights major differences between the Sf-rhabdoviral variants isolated by different investigators and/or harbored by different Sf cell lines. The major differences relevant to this study include 6 bp indels in the L coding sequence, which are indicated by a thick black line in the box representing the L coding sequence and labeled with the deleted (−) or inserted (+) sequences, and a 320 bp deletion spanning a portion of the X coding sequence and X/L intergenic region, which is indicated by a shorter box representing the X coding sequence and labeled as Delta;320 bp. The nucleotide numbers marking the start and end of each open reading frame are labeled above and below the boxes representing the coding sequences, respectively, except in the Sf9$^{L5814}$ map, for which the complete sequence was unavailable. (A) Sf9-rhabdovirus X$^{+}$L$^{Indel\text{-}I}$ refers to the variant originally identified in Sf9 cells by Ma and coworkers (2014), (B) Sf9-rhabdovirus X$^{-}$L$^{Indel\text{-}I}$ refers to the variant identified in Sf9 cells by Haynes (2015), (C)

$Sf9^{L5814}$-rhabdovirus $X^{-}L^{?}$ refers to the variant identified in $Sf9^{L5814}$ cells by Hashimoto and coworkers (2017), (D) Sf9-rhabdovirus $X^{-}L^{Indel\text{-}I}$ refers to the variant identified in Sf9 cells in the present study, (E) Sf21-rhabdovirus $X^{+}L^{Indel\text{-}II}$ refers to the variant identified in Sf21 cells by Ma and coworkers (2014), as well as in the present study.

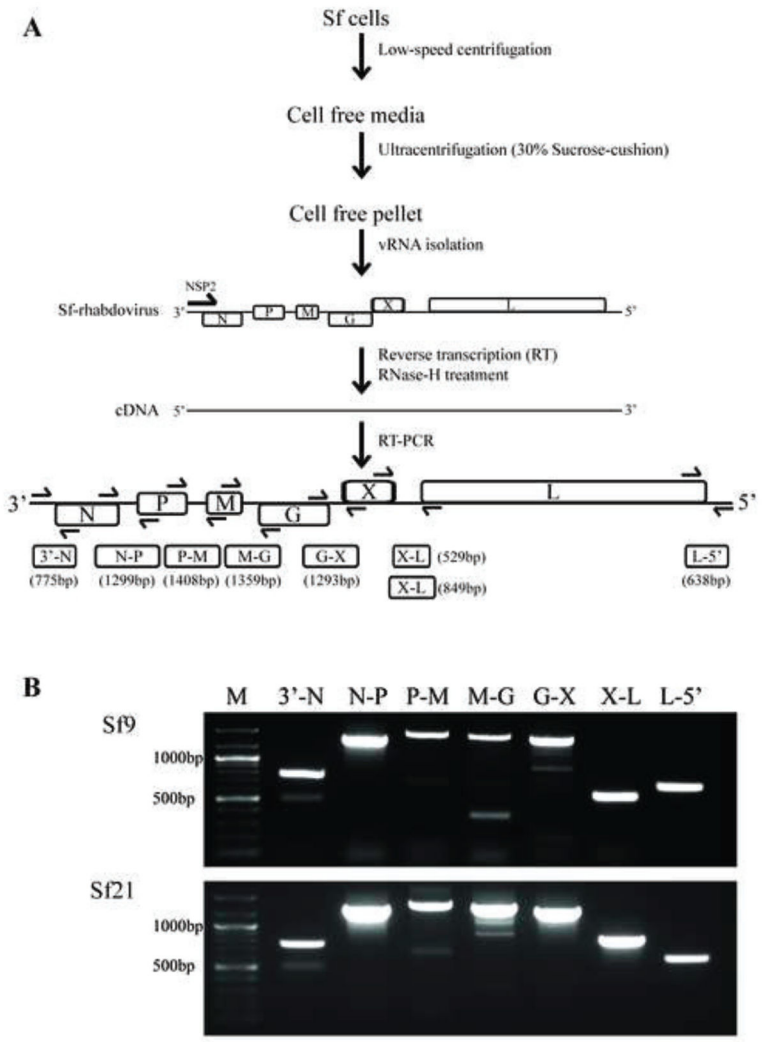


**Fig. 2.**

Sf-rhabdovirus negative stranded RNAs in the particulate fraction of various Sf cell-free media filtrates. (A) Method used to analyze the particulate fraction of various Sf-cell free media filtrates for Sf-rhabdoviral negative stranded RNA sequences by RT-PCR. One key feature of our assay was the use of NSP2, an Sf-rhabdovirus negative-stranded RNA-specific primer for the reverse transcription step, which was designed to exclusively amplify negative stranded RNAs. Another was the use of primer pairs specific for sequences flanking each intergenic region in the Sf-rhabdovirus genome, which was designed to enhance our effort to exclusively amplify negative-stranded RNAs, as the adjacent viral regulatory elements and/or coding sequences in those RNAs, but not positive stranded RNAs, would be linked. The amplification products expected from each primer pair are illustrated as 3'-N, N-P, P-M, M-G, G-X, X-L, and L-5', with predicted sizes indicated in parentheses. (B) Results of the RT-PCR assays performed using the particulate fractions of Sf9 or Sf21 cell-free media filtrates with the indicated primers. The lane marked M shows the 100-bp markers, with selected sizes indicated on the left.

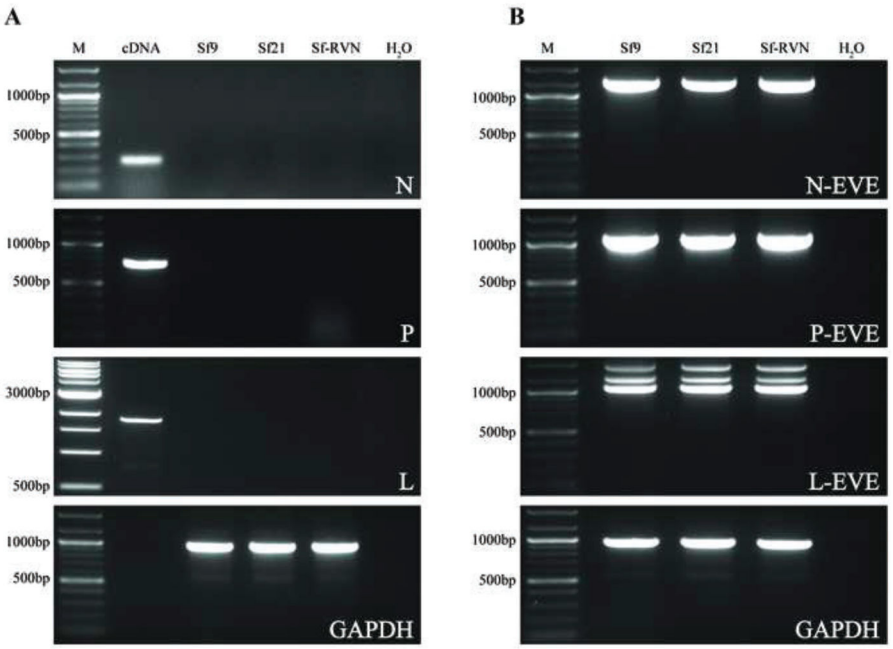


**Fig. 3.**

Genomic integration of Sf-rhabdovirus and Sf-rhabdovirus-related EVE sequences. Genomic DNAs were isolated from Sf9, Sf21, and Sf-RVN cells, as described previously (Geisler and Jarvis, 2016) and used for PCRs with (A) Sf-rhabdovirus N-, P-, or L-specific or (B) Sf-rhabdovirus N-, P-, or L-related EVE-specific primers, as described in Materials and methods. PCRs with no template ($H_2O$) were used as negative controls and PCRs with the indicated templates and Sf glyceraldehyde phosphate dehydrogenase (GAPDH)-specific primers were used as positive controls. PCRs with total Sf cellular cDNA as the template and the Sf-rhabdovirus N-, P-, and L-specific primers were used as an additional positive control in panel A. Note we did not include a cDNA template control in the GAPDH primer set, so no sample was loaded into the lane marked cDNA in the lowermost panel of A. The lane marked M shows the 100-bp or 1000-bp markers, with selected sizes indicated on the left.

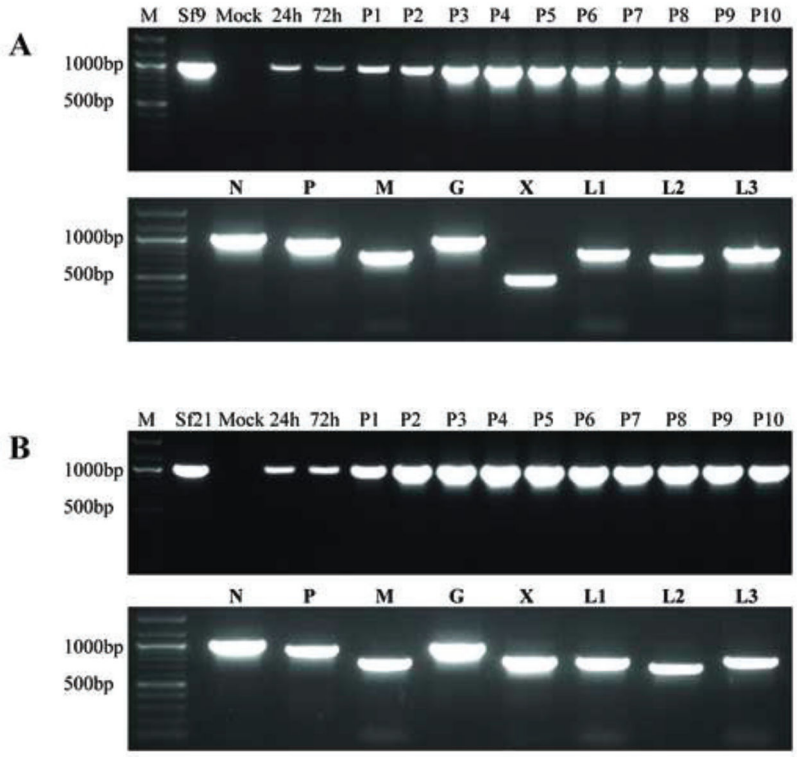


**Fig. 4.**

Infectivity of representative Sf-rhabdovirus variants in Sf-RVN cells. Sf-RVN cells were inoculated with fresh C-TNMFH (Mock) or C-TNMFH media filtrates from (A) Sf9 or (B) Sf21 cells. Total RNA was isolated from cell extracts prepared at various times and passages after inoculation and assayed by RT-PCR using N-specific primers (upper panels), as described in Materials and methods. In addition, total RNA was isolated from the particulate fraction prepared from the cell-free media filtrates at passage ten and assayed by RT-PCR using primers specific for various Sf-rhabdovirus coding sequences (lower panels), as described in Materials and methods. Total RNA extracted from the Sf9 or Sf21 cells used as the source of the inocula were used as positive controls for the RT-PCR assays. The lane marked M shows the 100-bp markers, with selected sizes indicated on the left.

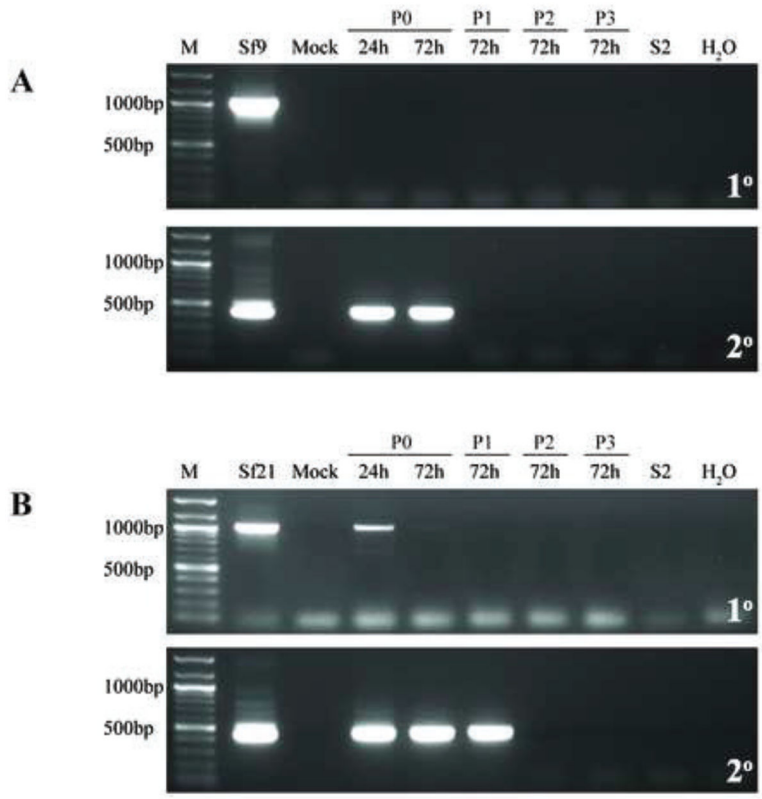


**Fig. 5.**

Infectivity of representative Sf-rhabdovirus variants in TN-368 cells. TN-368 cells were inoculated with fresh C-TNMFH (Mock) or C-TNMFH media filtrates from (A) Sf9 or (B) Sf21 cells. Total RNA was isolated from cell extracts prepared at various times and passages after inoculation and assayed by primary RT-PCR using N-specific primers (upper panels), as described in Materials and methods. In addition, the RT-PCRs were extended to include a secondary, nested PCR with N-specific primers (lower panels), as described in Materials and methods. RT-PCRs containing total RNA extracted from the Sf9 or Sf21 cells used as the source of the inocula were the positive controls and reactions containing total RNA extracted from S2R+ cells or no template ($H_2O$) were the negative controls. The lane marked M shows the 100-bp markers, with selected sizes indicated on the left.

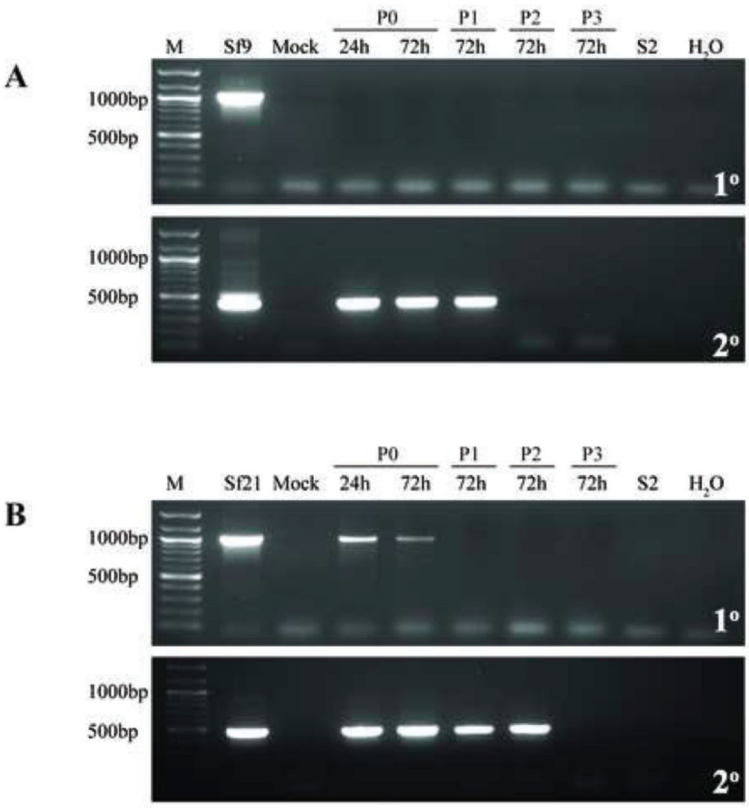


**Fig. 6.**

Infectivity of representative Sf-rhabdovirus variants in S2R+ cells. S2R+ cells were inoculated with fresh C-TNMFH (Mock) or C-TNMFH media filtrates from (A) Sf9 or (B) Sf21 cells and total RNAs were isolated from cell extracts at various times and passages after inoculation and assayed by primary RT-PCR (upper panels) and RT-PCR/nested PCR (lower panels) using N-specific primers, as described in the legend to Fig. 5. Positive and negative controls for the RT-PCRs were also performed as described in the legend to Fig. 5 and the lane marked M shows the 100-bp markers, with selected sizes indicated on the left.

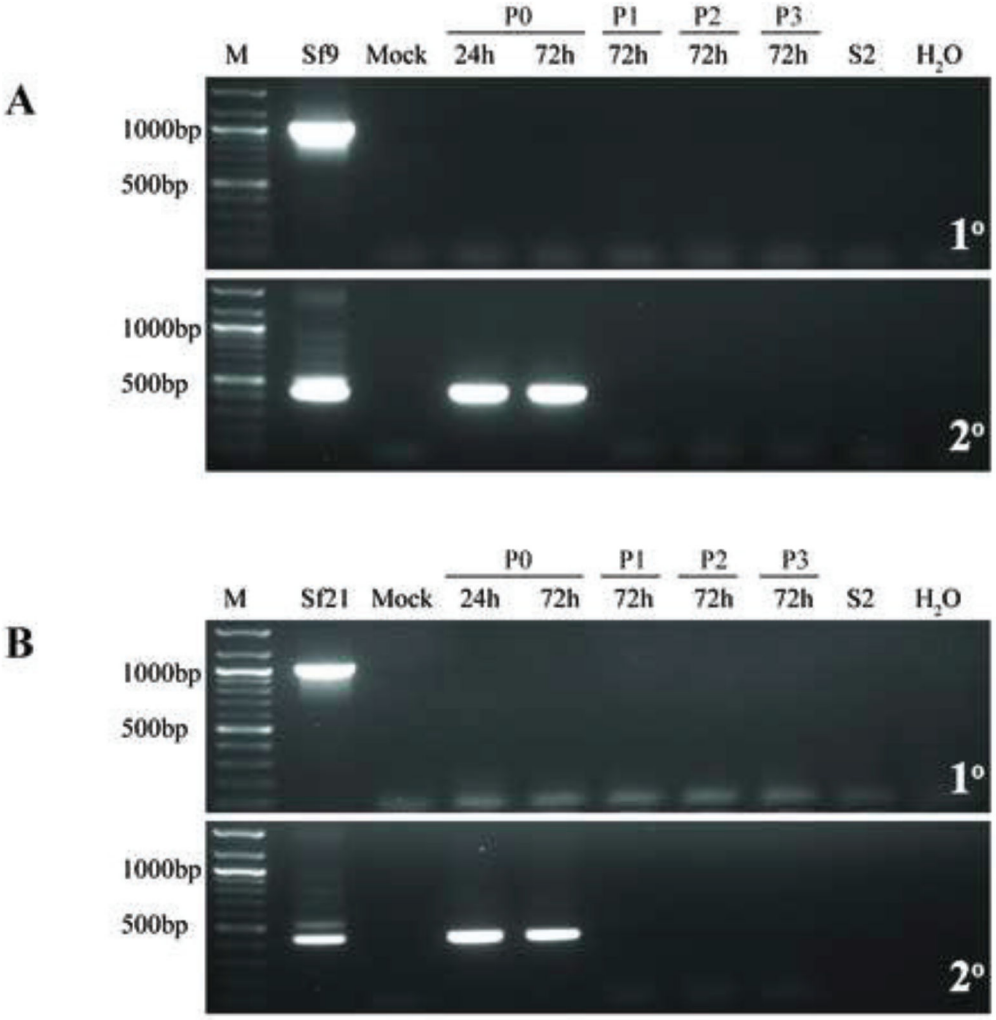


**Fig. 7.**

Infectivity of representative Sf-rhabdovirus variants in MDBK cells. MDBK cells were inoculated with fresh C-TNMFH (Mock) or C-TNMFH media filtrates from (A) Sf9 or (B) Sf21 cells and total RNAs were isolated from cell extracts at various times and passages after inoculation and assayed by primary RT-PCR (upper panels) and RT-PCR/nested PCR (lower panels) using N-specific primers, as described in the legend to Fig. 5. Positive and negative controls for the RT-PCRs were also performed as described in the legend to Fig. 5 and the lane marked M shows the 100-bp markers, with selected sizes indicated on the left.

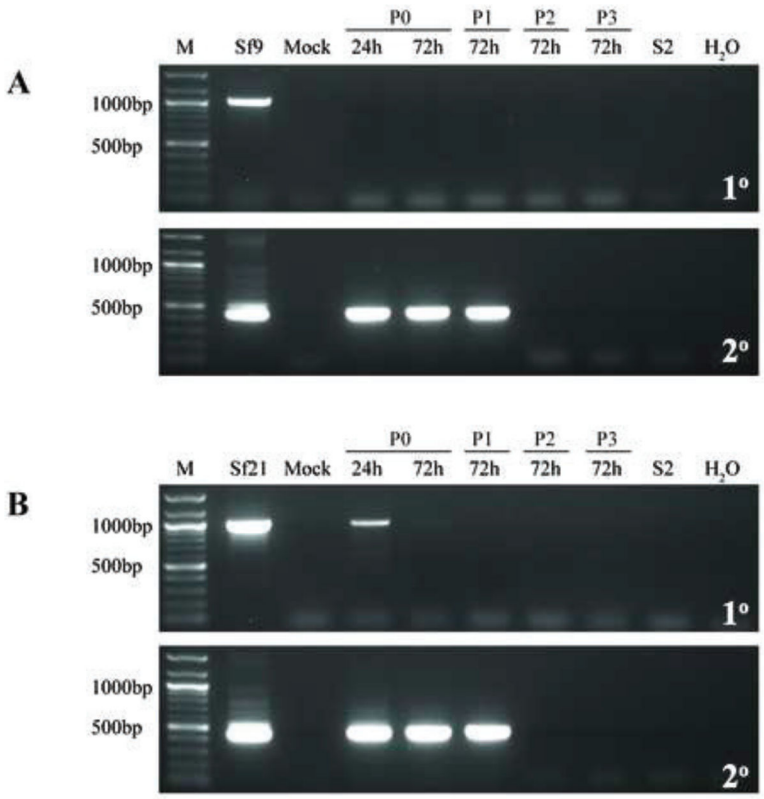


**Fig. 8.**

Infectivity of representative Sf-rhabdovirus variants in HeLa cells. HeLa cells were inoculated with fresh C-TNMFH (Mock) or C-TNMFH media filtrates from (A) Sf9 or (B) Sf21 cells and total RNAs were isolated from cell extracts at various times and passages after inoculation and assayed by primary RT-PCR (upper panels) and RT-PCR/nested PCR (lower panels) using N-specific primers, as described in the legend to Fig. 5. Positive and negative controls for the RT-PCRs were also performed as described in the legend to Fig. 5 and the lane marked M shows the 100-bp markers, with selected sizes indicated on the left.

## Table 1

Sequences of primers used in this study[1].

| Primer | Sequence (5'-3') | Position[2] | Product size[3] | Target |
|---|---|---|---|---|
| **NSP2** | TGA AAA TTA TAC GAT AAA TG | 1-20 | 775 | 3' – N |
| **Nseq2** | GTA GTA GCC TTT GCA ACA | 758-775 | | |
| **NSeq3** | GGA ATG GGG ATT TTA CAT G | 1143-1161 | 1299 | N – P |
| **PSeq2** | GCT GTA TAA GCA GTC ATA CC | 2422-2441 | | |
| **PSeq1** | GAA CTT ATA GAC ATC TGT C | 2194-2212 | 1408 | P – M |
| **MSeq2** | GCA AGC TGT ATC TCT GGT | 3584-3601 | | |
| **Mseq1** | GAT GGA TCC TGC ATC AAC | 3448-3465 | 1359 | M – G |
| **GSeq2** | GAG GGC AGC TAG ATT CTC | 4789-4806 | | |
| **GSeq3** | GCA TCC GGG TCG TGA AAG | 5036-5053 | 1293 | 1293G – X |
| **320-Seq1** | GGC TGT GAT GGT AGG TTT G | 6310-6328 | | 1293G – X |
| **320SP2** | ACC ATC ACA GCC AGT GCT G | 6317-6335 | 849/529[4] | X – L |
| **PCR2ASP** | GAG AAC CCC TTC AAC TTC | 7148-7165 | | |
| **LSeq9** | GGA TAC AAT GTG AGA ATG G | 12897-12915 | 638 | L – 5' |
| **LASP** | TAG ATC GTG GGG GAG GGG | 13517-13534 | | |
| **NSP** | GAG TGT TGA TAC ATG TCG | 194-211 | 1020 | N (1° PCR) |
| **NASP** | GTG ACC AAC CTC TTC CAG | 1196-1213 | | |
| **NSeq1** | GCC ACA GAA ATT GTA CTC TC | 330-349 | 446 | N (2° PCR) |
| **Nseq2** | GTA GTA GCC TTT GCA ACA | 758-775 | | |
| **PSP** | GCT CTA GTG TGC GAC TGT G | 1801-1819 | 936bp | P |
| **PASP** | GCT CAG ACA GGT TCT TAT TG | 2718-2737 | | |
| **MSP** | GTT GAA CCC TAG GAG AAC TC | 3132-3135 | 755bp | M |
| **MASP** | GTA TGC AGG TGG TTG AGG | 3870-3887 | | |
| **GSP** | GCT CCA ATC CTC TCT CCT AT | 4198-4217 | 972bp | G |
| **GASP** | GAC TGA GAG GGA ACT CAA | 5152-5169 | | |
| **320-SP1** | CAC ATC TAG AGC TTG AAG ACC | 6210-6230 | 801/481[4] | X |
| **320-ASP1** | GAA GTT GTC TCT GCA TCT CC | 6991-7010 | | |
| **Mono-1** | GGC AAG GCT GTT TGG ATT ACT GAC C | 8365–8389 | 794 | L1 |
| **Mono-2** | ACA GGT TTG CAG CTA AGG AGG ACA | 9158–9135 | | |
| **Mono-3** | TGG CGA GGG ACT GCT TAC AGA AGG | 10630–10653 | 730 | L2 |
| **Mono-4** | CAC AGC CGG GGG TGC AAT CA | 11359–11340 | | |
| **Mono-5** | ACA GGA GAT GCG GAA GAC CCC TC | 12137–12159 | 826 | L3 |
| **Mono-6** | ATC TCG CAG GTG GGA CAA CCC C | 12962–12941 | | |
| **N PSCF1** | GAT CCT AAC TCT TAT AGA TG | 20-39 | 273 | N[5] |
| **N PSCR1** | GTA AGA AAT CTG TTG AAG AT | 273-292 | | |
| **P PSCF1** | GAG GAG ATC TGA GTG GAA | 2123-2140 | 732 | P[5] |
| **P PSCR1** | GAT TGG TAA GAT CTG GGA | 2837-2854 | | |
| **L PSCF1** | GGC AAG GCT GTT TGG ATT ACT GAC C | 8365–8389 | 1847 | L[5] |
| **L PSCR1** | GAG AAT TTC CTG CAA CAT CT | 10192-10211 | | |
| **N EVEF1** | ACG GTT GGT CAC CAC AGG | | 1214 | N[6] |

| Primer | Sequence (5'-3') | Position[2] | Product size[3] | Target |
|---|---|---|---|---|
| **N EVER1** | GGC AAC CAC AGT GGA TCG | | | |
| **P EVEF1** | CTA CTG ACC CTG CCA TCG | | 1084 | P[6] |
| **P EVER1** | GGT TAA GCC TTC ACC CAC | | | |
| **L EVEF1** | CAG GAC AGA CAT CGG GTG | | 1076 | L[6] |
| **L EVER1** | CAC GTG GAT GGA GCA CAG | | | |
| **SfGAPSP** | TCG GTA TCA ACG GTT TCG | | 960 | GAPDH |
| **SfGAPASP** | GAT CGA TAA CGC GGT TGG | | | |

[1] Mono- primers were adapted from Ma et al. (2014).

[2] Numbers refer to starting and ending nucleotides in Sf-rhabdovirus reference sequence (GenBank Acc. No. KF947078).

[3] Indicates size of amplification products resulting from PCR with odd/even primer pairs.

[4] Size of amplification products depends on the presence or absence of 320 bp in X/L region.

[5] Sf-rhabdovirus-specific sequences detected in the Sf9L5814 cell genome (Hashimoto et al., 2017).

[6] Sf-rhabdovirus-related EVE sequences described by Geisler and Jarvis (2016).

**Table 2**

Single nucleotide polymorphisms (SNPs) in Sf-rhabdovirus variants.

| Viral Gene | Ref. Seq. Position (Acc. No. KF947078) | Sf9 | Sf21 | Viral Gene | Ref. Seq. Position (Acc. No. KF947078) | Sf9 | Sf21 |
|---|---|---|---|---|---|---|---|
| N coding | A333 | - | A333G | G coding | G4529 | - | G4529A |
| | A338 | - | A338C | | G4530 | - | G4530A |
| | C530 | - | C530A | | G4531 | - | G4531A |
| | C610 | - | C610T | | G4534 | - | G4534A |
| | C670 | C670T | - | | G4536 | - | G4536A |
| | C964 | C964T | - | | G4545 | - | G4545A |
| | A1040 | - | A1040C | | G4908 | - | G4908A |
| | C1095 | C1095T | C1095T | | G5036 | - | G5036A |
| | C1351 | - | C1351A | | A5147 | - | A5147C |
| | A1360 | A1360G | - | | G5392 | - | G5392T |
| | A1584 | - | A1584G | | A5817 | - | A5817G |
| | A1596 | - | A1596G | X coding | C6333 | C6333A | C6333A |
| | G2011 | - | G2011A | | A6354 | A6354T | - |
| | G2111 | G2111A | - | | C8052 | - | C8052T |
| P coding | A2311 | - | A2311G | | G8070 | - | G8070A |
| | A2588 | - | A2588C | | G8104 | G8104T | G8104T |
| | C2714 | - | C2714T | | A8524 | - | A8524G |
| | C2777 | - | C2777T | | T8713 | T8713C | - |
| P/M Intergenic Region | C2896 | - | C2896A | L coding | C8904 | - | C8904T |
| | T2926 | - | T2926G | | T9624 | T9624A | - |
| | A3155 | - | A3155G | | A9844 | - | A9844C |
| M coding | C3164 | C3164T | C3164T | | A10075 | - | A10075T |
| | C3206 | - | C3206T | | G10138 | - | G10138C |
| | T3285 | - | T3285G | | G11443 | G11443A | G11443A |
| | C3491 | C3491T | - | | T11514 | - | T11514C |
| | T3592 | - | T3592C | | C11602 | C11602T | - |
| | T3881 | - | T3881C | | T12407 | T12407C | T12407C |
| | A4251 | - | A4251G | | G12431 | - | G12431T |

| Viral Gene | Ref. Seq. Position (Acc. No. KF947078) | Sf9 | Sf21 | Viral Gene | Ref. Seq. Position (Acc. No. KF947078) | Sf9 | Sf21 |
|---|---|---|---|---|---|---|---|
| G coding | T4379 | - | T4379A | | C12544 | C12544A | - |
| | T4394 | - | T4394C | | | | |